

First in-situ evidence of solar wind acceleration

Consuelo Cid (✉ consuelo.cid@uah.es)

Universidad de Alcala

Carlos Larrodera

Universidad de Alcala

Manuel Flores-Soriano

Universidad de Alcala

Physical Sciences - Article

Keywords:

Posted Date: June 16th, 2022

DOI: <https://doi.org/10.21203/rs.3.rs-1758156/v1>

License:   This work is licensed under a Creative Commons Attribution 4.0 International License.

[Read Full License](#)

First in-situ evidence of solar wind acceleration

Carlos Larrodera, Consuelo Cid* and Manuel Flores-Soriano

Affiliations: **Space Weather Research Group, Physics and Mathematics Department, Universidad de Alcalá, Alcalá de Henares, Spain.**

Contributions: **All authors contributed equally to this work.**

*Corresponding author: **Correspondence to consuelo.cid@uah.es**

Abstract

Physical processes involved in the acceleration of stellar winds are essential in astrophysics as such winds are a mass loss process for stars. Hypothesis for stellar winds are difficult to check with experimental data in any other star but the Sun and even the processes of solar wind dynamics are poorly understood. Since the proposal by Parker of the stationary expansion of the solar atmosphere, the existence of the solar wind has been extensively demonstrated from data acquired from different missions in the Heliosphere. However, in-situ data showing that solar wind accelerates with the distance were still missing. Here we show the evolution of the solar wind speed distribution function with the heliocentric distance from $16 R_{\odot}$ to $172 R_{\odot}$ using Parker Solar Probe data. We observe that solar wind is accelerated until at least $60 R_{\odot}$, more than $20 R_{\odot}$ away than expected from previous studies. Below $\sim 25 R_{\odot}$ the subalfvenic wind dominates and is negligible from $35 R_{\odot}$ onwards. Here we find that the slow and fast winds are as mixed in the distribution function below $25 R_{\odot}$ as at 1 AU. Our findings provide empirical support for the models of solar wind dynamics.

Main

In 1958 Parker¹ theoretically formulated the existence of the solar wind concluding that the solar corpuscular radiation and the solar corona –or, indeed, the atmosphere of any star² were the same thing. Several measurements acquired since that time have proved the existence of the solar wind³. They have also allowed to check physical assumptions regarding the solar wind dynamics^{4,5}. The initially proposed stationary spherical expansion of an isothermal atmosphere provided a physical solution for the solar atmosphere corresponding to an outward expansion that becomes supersonic at the critical radius ($\sim 6 R_{\odot}$ for coronal conditions). Atmospheric heating, initially assumed by thermal conduction, was of primary importance in the behavior of an atmosphere. However, purely conductive models were ruled out to explain the high-speed solar wind observed near Earth ($>700 \text{ km s}^{-1}$), and that originates in coronal holes^{6,7}. The real corona was also discovered to be far from being spherically symmetric. Waves, turbulence and other heating and acceleration processes were proposed to explain the expanding solar wind. Besides, the physical mechanisms that operate on solar wind formation and evolution through the heliosphere are still an open question. The solar wind is usually observed in two states⁸: a thermally driven wind and a magnetically accelerated high-speed wind, where the magnetic field plays a substantial role in the acceleration of this fast wind.

The Parker Solar Probe (PSP) mission⁹ was launched in 2018 to reach closer to the Sun than any other spacecraft ever and to directly measure solar wind acceleration and heating processes below $20 R_{\odot}$. Previous in-situ measurements of the inner heliosphere were only provided by Helios 1 and Helios 2 space probes within heliocentric distances (r) of 0.29 to 0.98 AU. These measurements allowed to derive an empirical solar wind model for the inner heliosphere at the ecliptic, including solar activity and solar distance dependence, useful to estimate the solar wind environment for PSP planned trajectory¹⁰. The extrapolation of this model indicates that the solar wind average speed decreases from values of 340 km s^{-1} at $r = 0.25 \text{ AU}$ ($\sim 54 R_{\odot}$) to 290 km s^{-1} at $r = 0.046 \text{ AU}$ ($\sim 10 R_{\odot}$).

The solar wind speed profile at $r < 30 R_{\odot}$ is also measured by tracking the continuous outflow of material in the streamer belt appearing in white-light images from the LASCO/SOHO coronagraph during solar minimum¹¹. The moving coronal features - assumed as inhomogeneities in the solar wind- moved radially outward, increasing their speeds from 150 km s^{-1} near $5 R_{\odot}$ to $\sim 380 \text{ km s}^{-1}$ near $30 R_{\odot}$. Moreover, the speed profiles of the moving coronal features showed a constant acceleration of about 4 m s^{-2} through most of the $30 R_{\odot}$ field of view, consistent with an isothermal solar wind expansion at a coronal temperature of $1.1 \times 10^6 \text{ K}$ and a sonic point near $5-6 R_{\odot}$ ^{11, 12}.

The Wang Sheeley Arge (WSA)-ENLIL solar wind model^{13, 14} proposes that most of the change in solar wind speed evolution occurs within the few tenths of an AU from the Sun¹⁵. The solar wind speed distribution function predicted by WSA-ENLIL does not vary much between 0.385 AU ($83 R_{\odot}$) and 1.0 AU , though the speed of the peak in the distribution increases from 445 to 460 km s^{-1} showing a slight overall acceleration consistent with in-situ observations from Helios and L1 spacecraft. A very different picture emerges when they compare the speed distribution function at 1.0 AU to that at 0.1 AU : while at 1.0 AU resembles a Gaussian function, at 0.1 AU it is proposed to be very broad and flat across an extended range of solar wind speeds covering from 200 to 700 km s^{-1} ¹⁵.

For the first time PSP⁹ provides in-situ measurements within heliocentric distances of 16 to 172 R_⊙ ($\sim 0.07 - 0.8$ AU) allowing to investigate the continuous evolution of the solar wind speed from the most inner heliosphere until almost 1 AU on the ecliptic plane. To this end, we have computed the distribution function of the one-minute average radial solar wind speed data measured by the Solar Wind Electrons Alphas & Protons (SWEAP) instrument suite¹⁶ onboard PSP for several heliocentric distance intervals over the distance span of the dataset. A 2D color histogram of the distribution function mapping as a function of radial speed and heliocentric distance (Fig. 1) evidences the acceleration of the solar wind until at least 60 R_⊙. Moreover, the distribution function shifting towards larger speeds as the distance to the Sun increases (Fig. 2) can be observed until the interval ending at 105 R_⊙. Thus, our results demonstrate that the solar wind is accelerated up to $r \sim 60 - 100$ R_⊙, which is further away than the ~ 30 R_⊙ proposed in Parker's original solution¹ and currently used in solar wind models to forecast space weather¹⁵.

The new in-situ PSP data show that close to the Sun the solar wind velocity is lower than predicted by solar wind extrapolation¹⁰ and by the WSA-ENLIL model¹⁵ (see Fig. 1). The PSP observations also show that the distribution function at 0.1 AU (top panel in Fig. 2) has a peak at ~ 250 km s⁻¹ and a negligible contribution over 400 km s⁻¹, which is largely different to the WSA-ENLIL model solution¹⁵. Below 30 R_⊙ SWEAP/PSP data evidence a larger acceleration close to the Sun than that expected based on the observation of moving coronal features¹¹ (red curve in Fig. 1). The new data mostly agree with a $\square 300$ km s⁻¹ plateau, although starting at ~ 100 R_⊙ instead at ~ 20 R_⊙. SWEAP/PSP data also provide evidence that solar wind speed hardly reaches 300 km s⁻¹ before 30 R_⊙ (only 11% of data), contrary to LASCO observations of the white light corona¹⁷ which compare well with the classical solution¹² for a radially expanding isothermal corona at temperature of 10⁶ K.

Following an earlier approach¹¹, we fit the new data to a function of the form

$$v^2 = v_a^2 [1 - e^{-(r-r_1)/r_a}] \quad (1)$$

which approach an asymptotic speed v_a when $(r - r_1) \gg r_a$ (black curve in Fig. 1). The fitting results provide a value for $v_a = (330 \square 2)$ km s⁻¹, consistent with the value at 1 AU for slow solar wind¹⁸. At 30 R_⊙, when the solar wind was previously supposed¹¹ to flow at constant speed, we measure an acceleration of 1.8 m s⁻².

At the Earth orbit, the most probable value of the velocity (~ 380 km s⁻¹) is substantially lower than its median value (420 km s⁻¹), and the third and fourth moments of its distribution function are large¹⁹. This highly asymmetric frequency distribution of solar wind speed can be well approximated by two overlapping lognormal distributions¹⁰ or by a bi-Gaussian function¹⁸ where solar wind from different solar origin is mixed. Similar distribution functions to that at Earth orbit are observed at most radial distances (Fig. 2), contrary to the expectation of a more bimodal distribution close to the Sun^{15, 20}.

The distribution function in the interval 105 R_⊙ < r < 120 R_⊙ (blue line in the 7th panel of Fig. 2) departs from the shape followed by the distribution function at any other heliocentric distance. A peak appears in the distribution function of that interval (blue curve in 7th panel Fig. 2) with maximum at 427 km s⁻¹. It is associated with the passage of a fast stream from 17 to 21 May 2000, which contributes with about half of the data in the interval. The two clear peaks in the 105-135 R_⊙ interval could encourage us to

envison slow and fast wind as separate ones at that solar distance as expected for pristine solar wind²⁰. Nevertheless, the fact that the two different peaks are missing at shorter or larger heliocentric distances and the short percentage of data in this interval (1 %) lead us to conclude that this is a statistical effect. Indeed, after removing the data from the fast stream passage, the distribution function (in red in Fig. 2) has a similar shape as any other interval. Even though fast streams from coronal holes have been observed by PSP at other distances²¹, it is impossible to isolate the different types of wind in a smooth asymmetric function with a heavy tail which resembles that of the solar wind at 1 AU^{10, 15, 18, 19}. This result evidences the mixing and dynamical interaction of different types of wind also in the pristine solar wind.

A small enhancement in the distribution function from 16 R_☉ up to 30 R_☉ (top panel Fig. 2) is observed for speeds below 200 km s⁻¹. This enhancement disappears above 30 R_☉. To investigate this feature and how the distribution function evolves with heliocentric distance, we analyze smaller intervals of 5 R_☉ width from 20 R_☉ up to 45 R_☉, separating the contribution of the sub- (green) and superalfvenic (blue) wind. Subalfvenic wind disappears at heliocentric distances larger than 35 R_☉, clearly dominating until 25 R_☉. Moreover, subalfvenic contribution of the distribution function exhibits a shift towards higher speeds with heliospheric distance, indicating that it is being accelerated as it flows away.

Conclusions

Our results evidence the acceleration of the solar wind until ~60-100 R_☉, further away than expected from any theoretical model. Contrary to what past studies suggest, we find that the distribution function of the radial speed of pristine solar wind is like that at 1 AU showing a smooth asymmetric function with a heavy tail. This result is consistent with the mixing and dynamical interaction of different types of wind also close to the Sun. Furthermore, we find that the subalfvenic wind dominates until 25 R_☉ and its contribution is negligible from 35 R_☉ onwards. These observations point out that the critical radius may be further away from the Sun than expected.

Data availability

The raw data used in this work are publicly available via the Solar Parker Probe (<http://sweap.cfa.harvard.edu/pub/data/sci/sweap/>).

Code availability

The raw data were reduced and plots were generated using the public Python routines.

References

1. Parker, E. N. Dynamics of the interplanetary gas and magnetic fields. *Astrophys. J.* **128**, 664–676 (1958).
2. Vidotto, A. A. The evolution of the solar wind. *Living Rev Sol Phys* **18**, 3 (2021).
3. Neugebauer, M. and Conway, W. S. Mariner 2 observations of the solar wind: 1. Average properties. *J. Geophys. Res. Space Physics* **71**, 4469-4484 (1966).
4. Viall, N. M. and Borovsky, J.E., Nine Outstanding Questions of Solar Wind Physics. *J. Geophys. Res. Space Physics* **125**, e2018JA026005 (2020).

5. Bruno, R., Carbone, V. The Solar Wind as a Turbulence Laboratory. *Living Rev. Sol. Phys.* **10**, 1-208 (2013).
6. Krieger, A. S., Timothy, A. F., & Roelof, E. C. A coronal hole and its identification as the source of a high velocity solar wind stream. *Solar Physics* **29**, 505-525 (1973).
7. Kohl, J. L., Noci, G., Cranmer, S. R., & Raymond, J. C. Ultraviolet spectroscopy of the extended solar corona, *The Astronomy and Astrophysics Review*, **13**, 31-157 (2006).
8. Hollweg, J.V. The solar wind: Our current understanding and how we got here. *J Astrophys Astron* **29**, 217–237 (2008).
9. Fox, N.J., Velli, M.C., Bale, S.D. *et al.* The Solar Probe Plus Mission: Humanity’s First Visit to Our Star. *Space Sci Rev* **204**, 7–48 (2016).
10. Venzmer, M. S., & Bothmer, V. Solar-wind predictions for the Parker Solar Probe orbit-Near-Sun extrapolations derived from an empirical solar-wind model based on Helios and OMNI observations. *Astronomy & Astrophysics* **611**, A36 (2018).
11. Sheeley, N. R., Wang, Y. M., Hawley, S. H., Brueckner, G. E., Dere, K. P., Howard, R. A., ... & Biesecker, D. A. Measurements of flow speeds in the corona between 2 and 30 R_{\odot} . *The Astrophysical Journal*, *484*(1), 472 (1997).
12. Parker, E. N. Interplanetary dynamical processes. *New York* (1963).
13. Odstreil, D. Modeling 3-D solar wind structure. *Adv. Space Res.* **32**(4), 497–506 (2003).
14. Owens, M. J., H. E. Spence, S. L. McGregor, W. J. Hughes, C. N. Arge, P. Riley, J. A. Linker, and D. Odstreil, Metrics for solar wind pre-diction models: Comparison of empirical, hybrid, and physics-based schemes with 8 years of L1 observations. *Space Weather*, **6**, S08001, doi:10.1029/2007SW000380 (2008).
15. McGregor, S. L., *et al.* The radial evolution of solar wind speeds *Journal of Geophysical Research: Space Physics* **116**.A3 (2011).
16. Kasper, J. C. *et al.* Solar Wind Electrons Alphas and Protons (SWEAP) investigation: design of the solar wind and coronal plasma instrument suite for Solar Probe Plus. *Space Sci. Rev.* **204**, 131–186 (2016).
17. Wang, Y-M., *et al.* The dynamical nature of coronal streamers *Journal of Geophysical Research: Space Physics* **105**, A11 25133–25142 (2000).
18. Larrodera, C., and Cid, C. Bimodal distribution of the solar wind at 1 AU *Astronomy & Astrophysics* **635**, A44 (2020).
19. Veselovsky, I.S., Dmitriev, A.V. and Suvorova, A.V. Algebra and statistics of the solar wind. *Cosmic Res* **48**, 113–128 (2010).
20. Stansby, D., Horbury, T. S., & Matteini, L. Diagnosing solar wind origins using in situ measurements in the inner heliosphere, *Monthly Notices of the Royal Astronomical Society*, **482**, 1706–1714 (2018).
21. Karna, N., Berger, M. A., Asgari-Targhi, M., Paulson, K., & Fujiki, K. I. A Study of an Equatorial Coronal Hole Observed at the First Parker Solar Probe Perihelion. *The Astrophysical Journal*, **925**, 62–72 (2022).

Acknowledgements

We acknowledge the support by the MICINN (grant PID2020-119407GB-I00) and by the University of Alcalá (grant EPU_INV_UAH2021005). CL acknowledges FPI grant BES-2017-081533. Thanks to the Solar Wind Electrons, Alphas, and Protons (SWEAP) team

for providing data (PI: Justin Kasper, BWX Technologies) and thanks to the FIELDS team for providing data (PI: Stuart D. Bale, UC Berkeley). Parker Solar Probe was designed, built, and is now operated by the Johns Hopkins Applied Physics Laboratory as part of NASA's Living with a Star (LWS) program (contract NNN06AA01C). Support from the LWS management and technical team has played a critical role in the success of the Parker Solar Probe mission.

FIGURES

Figure 1. 2D color histogram of the distribution function of the radial solar wind speed measured by SWEAP/PSP. Heliocentric distances in top X-axis are in AU and in bottom one in solar radii. Black line corresponds to the fitting of PSP solar wind data to the equation (1). Also plotted are the heliocentric dependencies of the slow solar wind model from LASCO observations¹¹ (red line) and the extrapolation of the solar wind speed from Helios measurements to the PSP orbit region for slow and fast winds (green lines)¹⁰.

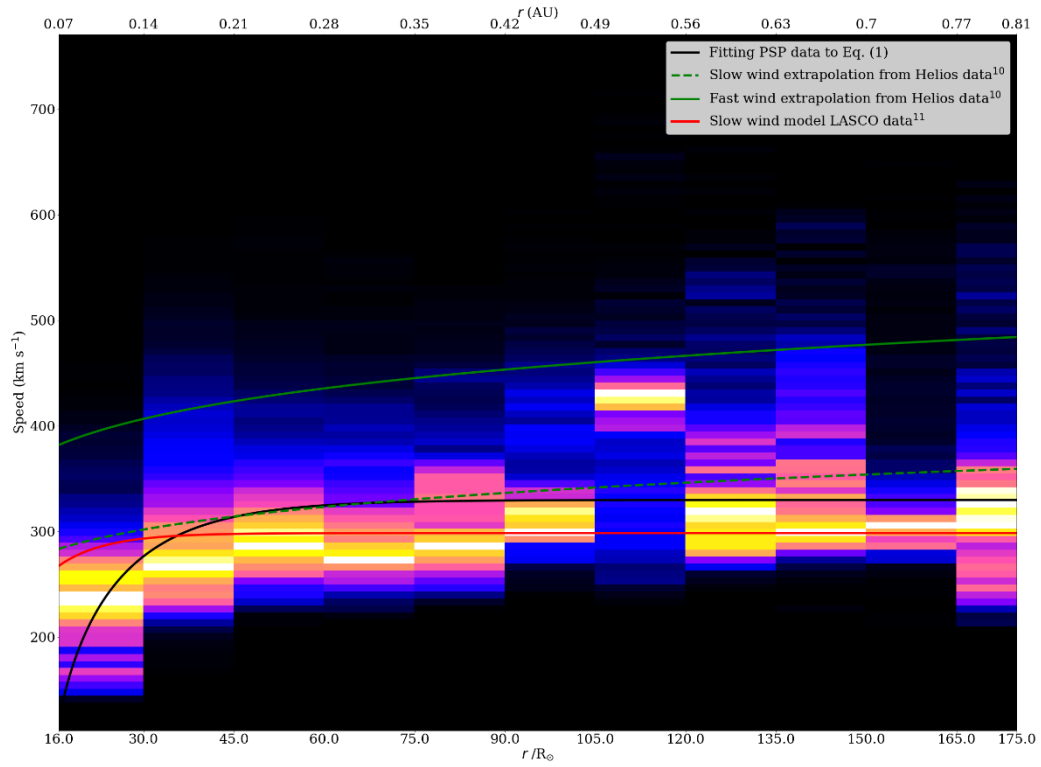


Figure 2. Distribution function of radial solar wind speed for selected intervals. Every panel includes in the top right the heliocentric distances covered and the percentage of the data of the whole sample contributing to this interval. The vertical axis range has been fixed in every panel considering the peak value of the distribution function in the corresponding interval. Red curve in panel $105 R_{\odot} < r < 120 R_{\odot}$ corresponds to the distribution function of a reduced data set (see text for details).

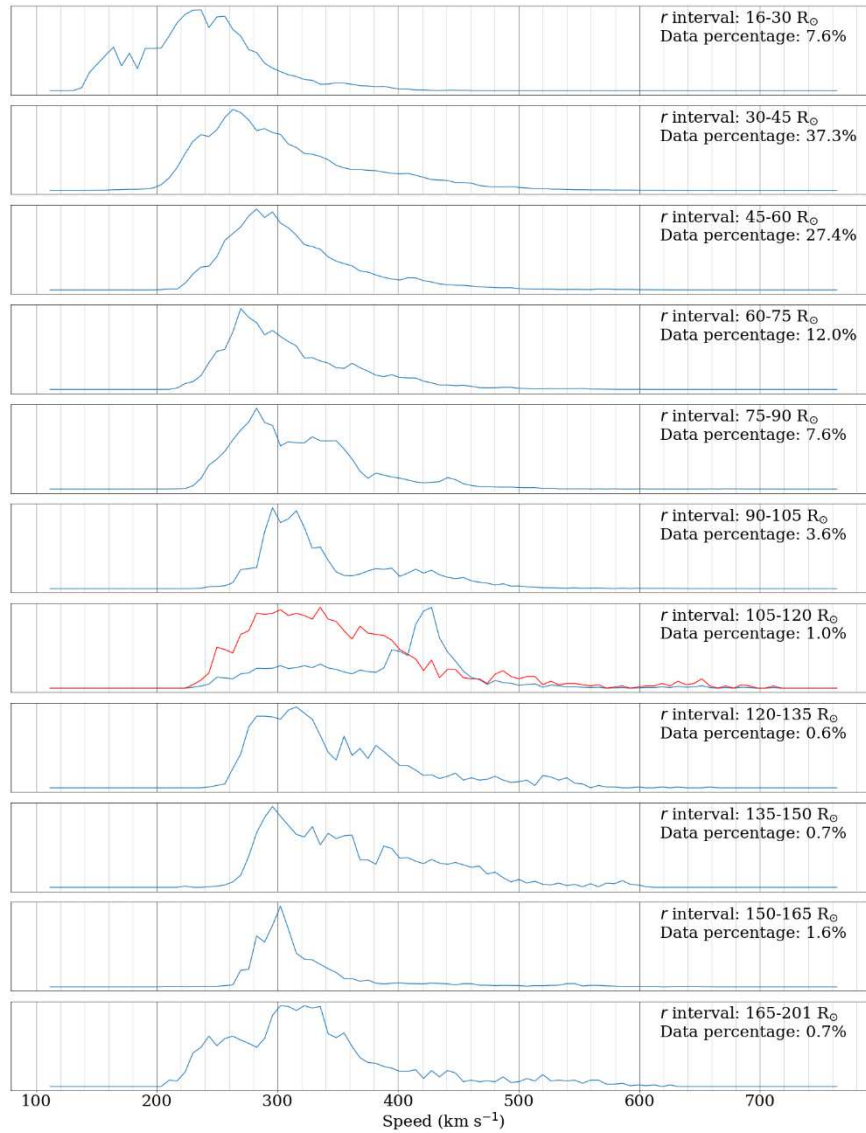


Figure 3. Distribution function of radial solar wind speed for selected intervals. Every panel includes in the top right the heliocentric distances covered and the percentage of the data relative to the whole data sample. Vertical axis indicate the number of counts. The same scale appears in all panels for comparison purposes. Green (blue) curves correspond to subalfvenic (superalfvenic) wind.

